



## Carbon dioxide vent for direct methanol fuel cells

Shruti Prakash, William Mustain, Paul A. Kohl\*

School of Chemical & Biomolecular Engineering, Georgia Institute of Technology, Atlanta, GA 30332, United States

### ARTICLE INFO

#### Article history:

Received 31 March 2008

Received in revised form 8 June 2008

Accepted 9 June 2008

Available online 26 June 2008

#### Keywords:

Methanol

Fuel cell

Membrane

Carbon dioxide

### ABSTRACT

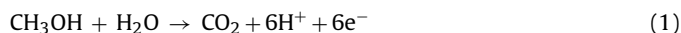
Passive, stand-alone, direct methanol fuel cells require a pressure management system that releases CO<sub>2</sub> produced in the anode chamber. However, this must be done without allowing the methanol fuel to escape. In this paper, two siloxane membranes are investigated and shown to selectively vent CO<sub>2</sub> from the anode chamber. The addition of hydrophobic additives, 1,6-divinylperfluorohexane and 1,9-decadiene, improved the selectivity of the siloxane membranes. The best performing CO<sub>2</sub> vent was obtained with 50:50 wt% poly(1-trimethyl silyl propyne) and 1,6-divinylperfluorohexane.

© 2008 Elsevier B.V. All rights reserved.

### 1. Introduction

Fuel cells are potentially a “green” power source with excellent energy density and the promise of scalability to small sizes. Fuel cells based on different technologies have been applied to various power levels including stationary power (100’s kW), transportation, and mini-power sources (1–5 kW) [1]. Recently, the use of fuel cells in small portable electronic devices, with power demands between 1 and 1000 μW has drawn much attention [2]. These electronic devices (e.g. sensors) require small size, good portability, and a high energy density. In larger fuel cells, the balance of plant components such as fuel pumps and humidifiers occupy a significant portion of the device volume and thus lowers the overall energy density of the unit.

To meet the high energy density requirement of portable wireless electronics, it is essential that the direct methanol fuel cell (DMFC) occupy the minimum possible volume. The principle of DMFC operation is based on catalytic redox reactions where methanol is oxidized to CO<sub>2</sub> at the anode, and O<sub>2</sub> is reduced to water at the cathode, as shown in the following equations, respectively:



In recirculating direct methanol fuel cells, peristaltic pumps are used for fuel (CH<sub>3</sub>OH and H<sub>2</sub>O) delivery at the anode field [3–8].

Alternatively, some studies have focused on delivering fuel to the anode with pipettes or feed tubes [9]. To reduce the fuel cell volume, the balance of plant components must be minimized through the use of a passive fuel delivery system.

The process of CO<sub>2</sub> discharge from the anode chamber without significant loss of methanol raises a key challenge in fuel cells designed with minimal volume and passive components. One mole of CO<sub>2</sub> is produced for each mole of methanol oxidized. Since CO<sub>2</sub> has limited solubility in methanol, CO<sub>2</sub> bubbles are formed at the anode and reduce the effective anode area, as studied by Yang et al. [10]. CO<sub>2</sub> buildup also causes an increase in pressure inside the DMFC fuel tank which will increase the fuel crossover problem and finally lead to tank or seal rupture. This issue becomes critical for all-passive fuel cells that strive for volumetric efficiency and have no pressure relief mechanism. To further understand the severity of CO<sub>2</sub> accumulation, consider a DMFC with 1 cm<sup>3</sup> head space in the fuel tank. If the cell operates at 20 μA current, and the CO<sub>2</sub> molecules were not vented, the overpressure inside the fuel tank would increase by about 1 psi day<sup>-1</sup> (7 kPa day<sup>-1</sup>).

Previous small DMFC studies have evaded this important issue of an efficient mechanism for CO<sub>2</sub> venting [4,11,12]. One approach to deal with the build-up of CO<sub>2</sub> is to design a mechanical pressure relief valve. However, the loss of methanol vapor, complexity of valve design, and space limitations make this approach undesirable. A selective membrane for separation of the carbon dioxide from methanol is preferred because of its size and simplicity. The mechanism of gas transport through polymeric membranes is governed by Knudsen diffusion, molecular diffusion or solution diffusion [13]. The transport of a gas molecule through a polymeric matrix depends on the proficiency of small penetrants to diffuse and per-

\* Corresponding author.

E-mail address: [Paul.Kohl@chbe.gatech.edu](mailto:Paul.Kohl@chbe.gatech.edu) (P.A. Kohl).

**Table 1**  
Permeability coefficient for CO<sub>2</sub> and O<sub>2</sub> in barrers

Polymer	Permeability coefficient at STP (barrers)	
	O <sub>2</sub>	CO <sub>2</sub>
Polyethylene	2.2	9.5
Natural rubber	24	131
Silicone rubber (PDMS)	540–600	3230
PTMSP	7725	28,000

meate in response to a gradient in the chemical potential [14,15]. According to Chandak et al., the transfer mechanism of volatile organic compounds (VOCs) through the membrane is governed by three separate physical processes: VOC sorption in the membrane at the upstream interface, propagation and diffusion through the bulk material of the membrane and finally desorption at the downstream interface of membrane [16]. The intermolecular attraction between different functional group segments, morphology, chain structure and rigidity of polymer backbone are few of the governing factors that affect the transport mechanism of a permeate through the polymeric membrane. Thus, by carefully controlling these factors, the transport behavior of a polymer membrane can be altered to meet the design requirements for gas separation [17].

In this work, the use of a polymer membrane for gas transport and CO<sub>2</sub>/methanol separation has been investigated. The design and operational parameters of a novel CO<sub>2</sub> venting technology for DMFCs using polymer membranes have also been described. The key parameter in the selective membrane is to maximize the transport of carbon dioxide with respect to methanol. The performance of two polymers: (i) poly(dimethyl siloxane) (PDMS) and (ii) poly(1-trimethyl silyl propyne) (PTMSP) have been investigated because of their hydrophobic nature, which supports the solubility of carbon dioxide over methanol. Compared to common polymeric materials (e.g. natural rubber and polyethylene), both PDMS and PTMSP are known to exhibit extremely high gas permeabilities. Table 1 compares the permeability coefficients of oxygen and carbon dioxide through natural rubber and polyethylene with PDMS and PTMSP membranes. The permeability coefficient of CO<sub>2</sub> through PDMS is 100 times higher than polyethylene and 30 times higher than natural rubber. The corresponding permeability coefficients through PTMSP are 1000–10,000 times higher than natural rubber or polyethylene. However, the transport of methanol through these membranes as well as their performance in the presence of a non-ideal of methanol and CO<sub>2</sub> has not been previously explored.

## 2. Theory

The permeability coefficient of a permeate (gas or vapor) through a polymer matrix can be estimated using the Nernst Distribution function [18–20]. The permeability coefficient of species *i*,  $P_i$ , is defined as the product of its diffusion coefficient ( $D_i$ ) and its solubility coefficient ( $S_i$ ) and is given as the following equation:

$$P_i = D_i S_i \quad (3)$$

Under steady-state conditions, the solubility of a material is fixed and the rate of permeate transport can be looked at as the flux of permeate through the solid polymer matrix. Therefore, the permeability coefficient of species *i* through a polymer matrix can be expressed using the following equation:

$$P_i = \frac{N_i l}{\Delta p A} \quad (4)$$

where  $N_i$  is the steady-state rate of mass transfer of species *i* through the polymer matrix,  $l$  is the thickness of the polymer mem-

brane,  $A$  is the area, and  $\Delta p$  is the pressure gradient of species *i* between the upstream and the downstream side. Since the permeability coefficient is an intrinsic property of the material, it represents a useful tool in comparing the performance of different permeates through a material. For the study of a CO<sub>2</sub> vent in a passive DMFC, a useful figure of merit is the ratio of the permeability coefficient of CO<sub>2</sub> ( $P_{CO_2}$ ) to methanol ( $P_{MeOH}$ ), denoted in the following equation by  $\alpha$ :

$$\alpha = \frac{P_{CO_2}}{P_{MeOH}} \quad (5)$$

Values of  $\alpha$  greater than 1 indicate that the membrane is intrinsically more selective to CO<sub>2</sub> than methanol. However,  $\alpha$  is not the absolute difference in CO<sub>2</sub> and methanol mass transport through the film because the composition or partial pressure of CO<sub>2</sub> and methanol are different in the fuel container and may change with time. This would lead to a different permeation rate, though the permeability coefficient, being an intrinsic property of the membrane, remains the same. As such, the selectivity of the membrane,  $S$ , is defined as the ratio of the absolutes rates of mass transport of CO<sub>2</sub> and methanol through the polymer film.

$$S = \frac{N_{CO_2}}{N_{MeOH}} = \alpha \left( \frac{\Delta p_{CO_2}(t)}{\Delta p_{MeOH}(t)} \right) \quad (6)$$

Assuming ideal gas behavior,  $S$  can be expressed in terms of the partial pressure of CO<sub>2</sub> ( $p_{CO_2}(t)$ ) and methanol ( $p_{MeOH}(t)$ ) in the fuel tank headspace. The resulting expression for  $S$  is given by the following equation:

$$S = \alpha \left( \frac{p_{CO_2}(t)}{p_{MeOH}(t)} \right) \quad (7)$$

Eq. (7) can be further simplified by assuming that the partial pressure of methanol in the headspace of a stand-alone DMFC is the same as the saturated vapor pressure, which occurs when the two phases are in equilibrium. Eq. (7) can be rewritten in terms of the saturated vapor pressure of methanol and the absolute pressure of CO<sub>2</sub> in the headspace as shown in the following equation:

$$S = \alpha \left( \frac{p_{CO_2}(t)}{p_{MeOH}^{sat}} \right) \quad (8)$$

While  $S$  represents a more useful diagnostic tool for the prepared films during operation,  $\alpha$  is a more convenient comparative tool between candidate materials for the CO<sub>2</sub> vent. Since the selectivity is directly related to the absolute rate of the permeate mass transport, we can define a fuel utilization efficiency,  $\gamma$ , as the ratio of the electrochemical consumption of methanol to total methanol consumption (methanol consumed via electrochemical reaction and methanol lost though the polymer vent permeation), as shown in the following equation:

$$\gamma = \frac{i/nF}{i/nF + N_{MeOH}} \quad (9)$$

Since the methanol consumed through the electrochemical reaction is stoichiometrically related to the CO<sub>2</sub> generated (Eq. (2)), the rate of CO<sub>2</sub> generation is equal to the CO<sub>2</sub> permeation rate through the vent under steady-state conditions, as shown in the following equation:

$$\gamma = \frac{N_{CO_2}}{N_{CO_2} + N_{MeOH}} = \frac{1}{(N_{MeOH}/N_{CO_2}) + 1} \quad (10)$$

Combining the definition of the selectivity, Eq. (6), with Eq. (10), yields a simple expression for the CO<sub>2</sub> vent efficiency, the following

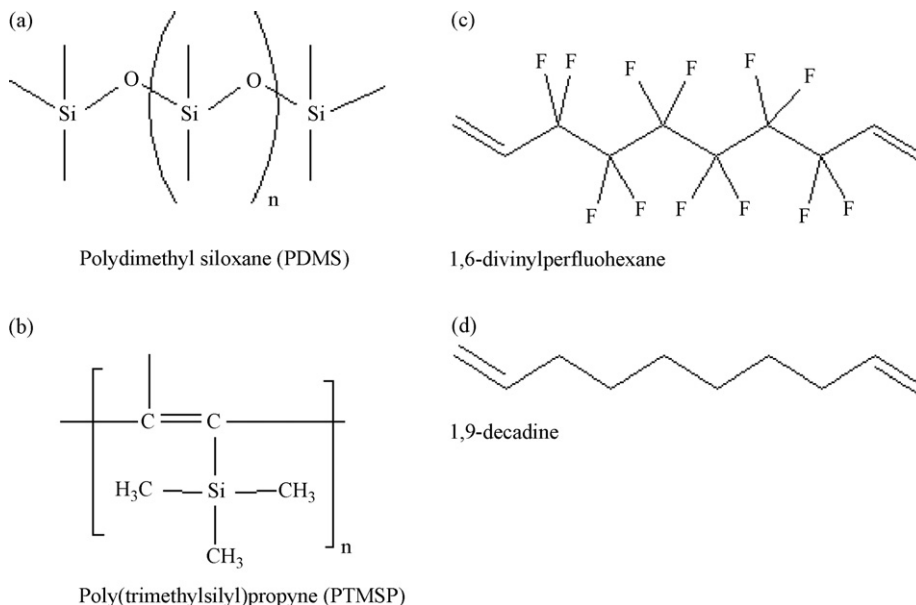


Fig. 1. Chemical structures of CO<sub>2</sub> vent candidate: (a) PDMS, (b) PTMSP, (c) 1,6-divinylperfluorohexane, and (d) 1,9-decadiene.

equation is obtained:

$$\gamma = \frac{S}{S+1} \quad (11)$$

### 3. Experimental

A two-part silicone elastomer (base and curing agent, SYLGARD) was obtained from Dow Corning to fabricate PDMS membranes. The elastomer curing agent was added to the base in a 1:10 (wt) ratio. This mixture was mechanically stirred for 30 min to ensure complete mixing. This was followed by a 1-h room temperature degassing step at 18 kPa absolute pressure in a vacuum oven (Isotemp Vacuum Oven, Model 281A). Once the mixture was degassed, it was spin coated on a Teflon substrate to form a thin film using a CEE-100 CB Spinner. The membrane was cured at 100 °C for 1 h (Fischer Scientific Isotemp Oven). The cured membrane was then peeled from the substrate.

PTMSP was obtained from Gelest Corporation. It was dissolved in toluene at room temperature, and mixed for 1 week using a rotary mixer. The amount of solvent in the polymer was adjusted to obtain a desired viscosity of the polymer mixture so as to facilitate spin coating. Thin films of the membrane were spin coated on a Teflon substrate. Slow evaporation of the solvent was achieved by placing the cast membrane under a pressure of 90 psia (600 kPa absolute) at 60 °C for 3 h. The resulting membranes were then peeled from the substrate.

In this study, two kinds of additives were incorporated into the PDMS and PTMSP membranes: 1,9-decadiene (Alfa Aesar) and 1,6-divinylperfluorohexane (97%) (Matrix Scientific). These additives were included in the polymer mixtures by mechanically mixing in different weight ratios prior to the curing step. Fig. 1 lists the chemical structure of PDMS and PTMSP along with the two additives mentioned above.

Contact angle measurements were conducted using the ACT video contact angle system (VCA 2500XE). All measurements were taken using DI water at room temperature. Two sets of experiments were conducted to measure the permeability coefficient of CO<sub>2</sub> and methanol through the polymer membranes. First, the permeability rate of CO<sub>2</sub> and methanol was measured independently of each

other and second, the permeability was measured when CO<sub>2</sub> and methanol were present together as a binary mixture. In each case, the thickness of the fabricated membranes was measured using precision calipers.

### 4. Results

The study of CO<sub>2</sub> and methanol permeation was carried out through two sets of experiments. In the first experimental setup, the permeation rates of methanol and CO<sub>2</sub> were measured independently. Methanol permeation studies were carried out by methanol gravimetric analysis as methanol was lost from a closed container through a membrane sealed onto a glass vessel. The rate of mass loss of methanol through the PDMS and the PTMSP membranes was recorded as a function of time. All measurements were made at STP. The PDMS membrane used in this experiment was 105 μm thick with an exposed area (to methanol) of 0.352 cm<sup>2</sup>. The thickness of the PTMSP membrane was 33 μm with an exposed area of 0.608 cm<sup>2</sup>. Fig. 2 shows the weight loss of methanol as a function of time through the PDMS and the PTMSP membranes. The curves shown in Fig. 2 reflect a linear relationship between weight loss and time, as expected under steady-state conditions for a fixed exposure area. The rate of methanol weight loss is

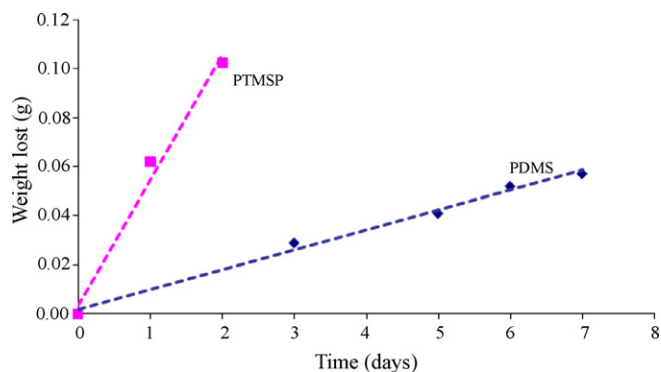
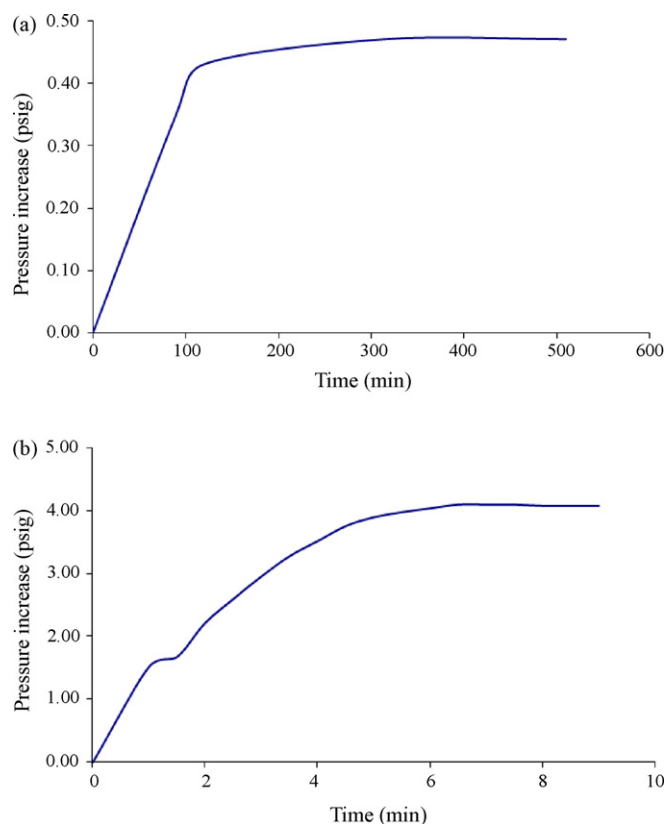


Fig. 2. Methanol loss as a function of time through a PDMS and PTMSP membrane.



**Fig. 3.** (a) Rate of pressure increase due to CO<sub>2</sub> permeation through PDMS membrane. (b) Rate of pressure increase due to CO<sub>2</sub> permeation through PTMSP membrane.

0.008 and 0.0512 g day<sup>-1</sup> through the PDMS and the PTMSP membranes, respectively. Using Eq. (4), the corresponding permeability coefficient of methanol is  $4.76 \times 10^{-10}$  mol cm cm<sup>-2</sup> day<sup>-1</sup> Pa<sup>-1</sup> through PDMS and  $5.1 \times 10^{-10}$  mol cm cm<sup>-2</sup> day<sup>-1</sup> Pa<sup>-1</sup> through PTMSP membranes.

CO<sub>2</sub> permeation studies were carried out by measuring the pressure increase due to CO<sub>2</sub> transport through a thin polymer film. The membrane was tightly sealed to a pressure chamber using an o-ring and clamp. The CO<sub>2</sub> which permeates through the membrane was captured in a closed chamber. The upstream pressure of CO<sub>2</sub> was maintained between 2 and 5 psig and the downstream pressure (of the sealed capture chamber) was recorded as a function of time at ambient temperature. The thickness of the PDMS membrane was 300 μm and the PTMSP membrane was 118 μm with an exposed area of 0.015 cm<sup>2</sup> for each. Fig. 3a and b shows the rate of pressure increase on the downstream side of the PDMS and the PTMSP membranes due to CO<sub>2</sub> permeation and accumulation in the sealed chamber. It is observed from Fig. 3a and b that the pressure of CO<sub>2</sub> on the downstream side increases until it reaches a steady-state value which is equal to the upstream pressure of CO<sub>2</sub> across the membrane. At this point, the CO<sub>2</sub> is in mechanical equilibrium across the membrane. The rate of pressure increase in the sealed chamber is calculated from the slope of the curve in Fig. 3 before it reaches steady-state conditions. For the PDMS membrane, the CO<sub>2</sub> pressure increases at an initial rate of  $9.21 \times 10^{-4}$  psi min<sup>-1</sup> and PTMSP at 0.631 psi min<sup>-1</sup>. The resulting permeability coefficient (Eq. (4)) of CO<sub>2</sub> was  $9.5 \times 10^{-10}$  and  $1.25 \times 10^{-9}$  mol cm cm<sup>-2</sup> day<sup>-1</sup> Pa<sup>-1</sup> for the PDMS and PTMSP membranes, respectively. Based on the permeability coefficients of methanol and CO<sub>2</sub> through the PDMS and the PTMSP membranes, the magnitudes of  $\alpha$  were estimated for each membrane using Eq. (5). A value of 1.98 for  $\alpha$  was obtained

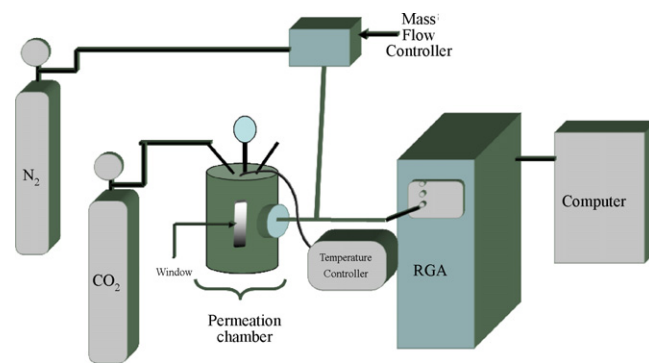


**Fig. 4.** Permeation cell setup.

for the PDMS membrane and the corresponding value of  $\alpha$  for the PTMSP membrane was 2.45.

The values of  $\alpha$  obtained from the independent experiment setup were promising; however,  $\alpha$  may vary under real operating conditions due to the non-ideal effects of having a methanol and CO<sub>2</sub> mixture. Therefore, to mimic the true polymer film performance and evaluate the permeability coefficients of CO<sub>2</sub> vent membranes, a permeation cell was constructed to house both methanol and CO<sub>2</sub>. This 'binary experiment' is shown schematically in Fig. 4. The upstream pressure of CO<sub>2</sub> inside the cell was maintained between 4 and 5 psig (28–32 kPa) and the gas inside the permeation cell was saturated with methanol at all times. On the exit or downstream side of the membrane, nitrogen was used as a sweep gas to carry permeates from the membrane to a quadrupole mass spectrometer. The rate of CO<sub>2</sub> and methanol permeation through a 255-μm thick PDMS membrane having an area of 2.85 cm<sup>2</sup> was measured. The relative amount of CO<sub>2</sub> and methanol detected as a function of time is shown in Fig. 5. The instantaneous flux of CO<sub>2</sub> and methanol through the membrane was calculated using mass spectrometry sensitivity factors, which were obtained under known flow rate conditions in separate experiments. The equivalent steady-state flux of CO<sub>2</sub> and methanol was  $4.2 \times 10^{-4}$  and  $5.96 \times 10^{-5}$  mol day<sup>-1</sup> cm<sup>-2</sup>, respectively. The resulting permeability coefficient of CO<sub>2</sub> and methanol through the PDMS membrane was  $1.6 \times 10^{-9}$  and  $9.05 \times 10^{-10}$  mol cm cm<sup>-2</sup> day<sup>-1</sup> Pa<sup>-1</sup>, respectively.

A similar permeation experiment was conducted for a 120-μm PTMSP membrane, with an area of 2.85 cm<sup>2</sup>. The relative amounts of methanol and CO<sub>2</sub> are shown in Fig. 6 as a function of time. The steady-state flux of CO<sub>2</sub> and methanol through PTMSP, calculated from Fig. 6, are  $4.91 \times 10^{-4}$  and  $1.12 \times 10^{-4}$  mol day<sup>-1</sup> cm<sup>-2</sup>,

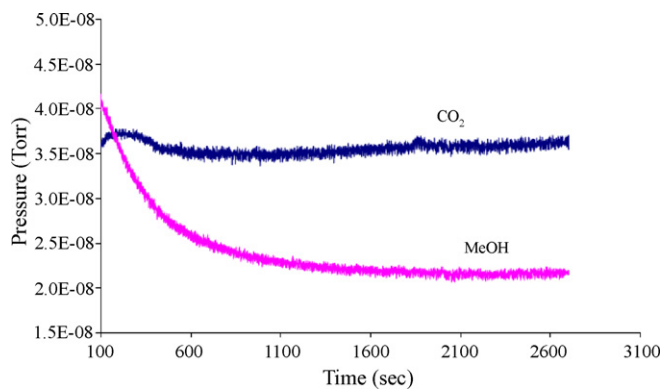


**Fig. 5.** Pressure signal detected by RGA for CO<sub>2</sub> and methanol through PDMS membrane.

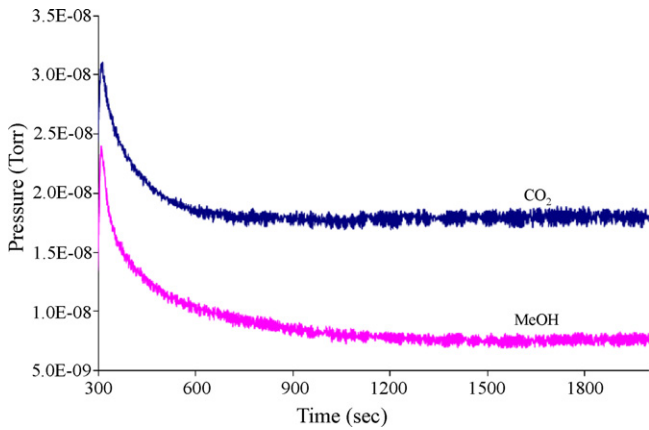


Fig. 6. Pressure signal detected by RGA for CO<sub>2</sub> and methanol through PTMSP membrane.

respectively. The corresponding permeability coefficients of CO<sub>2</sub> and methanol through the PTMSP membrane are  $1.7 \times 10^{-9}$  and  $8 \times 10^{-10}$  mol cm cm<sup>-2</sup> day<sup>-1</sup> Pa<sup>-1</sup>, respectively.

The values for  $\alpha$  were determined from the permeability coefficients of CO<sub>2</sub> and methanol through the PDMS and PTMSP membranes from their fluxes in separate permeation experiments and when mixed together. These values are shown in Table 2. In all cases, the permeability coefficients for CO<sub>2</sub> through the PDMS and the PTMSP membranes were higher than the permeability coefficients of methanol through the same materials. Also, PDMS has higher permeability for methanol than PTMSP. The value of  $\alpha$  was 1.98 through the PDMS and 2.45 through PTMSP as was obtained from the individual permeation experiments. The mass spectrometry results for the CO<sub>2</sub>–methanol mixtures yielded permeability coefficients and  $\alpha$  values in agreement with the separate-chemical experiments. The resulting  $\alpha$  values were 1.8 for PDMS membranes and 2.13 for PTMSP membranes.

As discussed previously,  $\alpha$  values greater than unity are desired,  $\alpha$  values greater than 1 indicates that both PDMS and PTMSP membranes are intrinsically more selective to CO<sub>2</sub> than methanol. Most likely the hydrophobicity of the PDMS and the PTMSP membranes leads to an increased transport of CO<sub>2</sub>, compared to methanol. To further increase the hydrophobicity of the PDMS and the PTMSP membranes, hydrophobic additives were incorporated into the polymer during membrane casting. To this end, two different additives, 1,6-divinylperfluorohexane and 1,9-decadiene, were used. Contact angle measurements were used to investigate the hydrophobic nature of the additives in the polymer matrix. Fig. 7 shows the water contact angles for PDMS and PTMSP membranes as a function of the weight percent of 1,6-divinylperfluorohexane in each polymer. As shown in Fig. 7, the contact angle increased with increasing amount of 1,6-divinylperfluorohexane in the polymer matrix showing the enhanced hydrophobic nature of the mixture.

To quantify the effect of hydrophobicity of the PDMS and PTMSP films on the separation performance with the two additives (1,6-divinylperfluorohexane and 1,9-decadiene), permeability

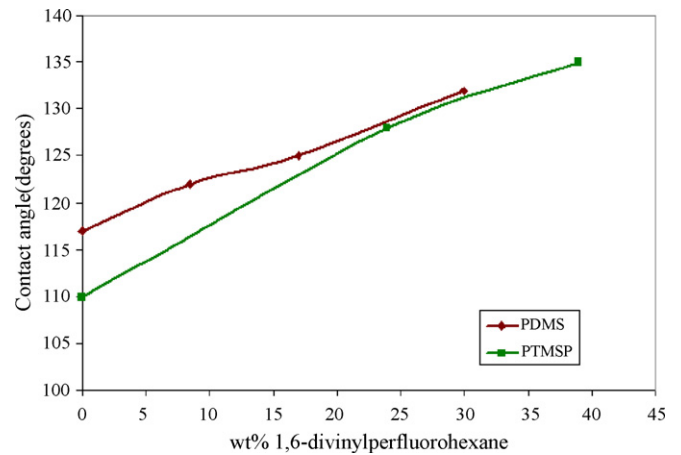


Fig. 7. Water contact angle measurement for PDMS and PTMSP as a function of 1,6-divinylperfluorohexane.

experiments were carried out for CO<sub>2</sub> and methanol, and their mixtures. Polymer membranes with an average thickness of 250  $\mu$ m were cast for the mixtures of 1,6-divinylperfluorohexane and PDMS. The flux of CO<sub>2</sub> and methanol were measured at ambient temperature across an area of 2.85 cm<sup>2</sup>. Using Eq. (4), the molecular fluxes were translated into a permeability coefficient as a function of the additive content. The corresponding values of  $\alpha$  were estimated from Eq. (5). Fig. 8a and b shows the permeability coefficients and  $\alpha$  for CO<sub>2</sub> and methanol as a function of 1,6-divinylperfluorohexane content in PDMS. The solid lines in Fig. 8a

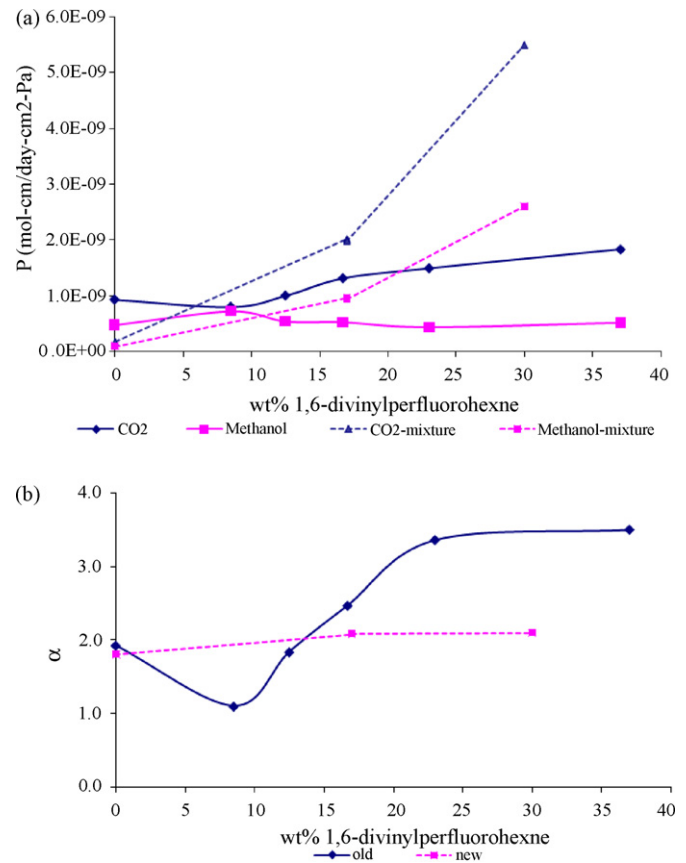
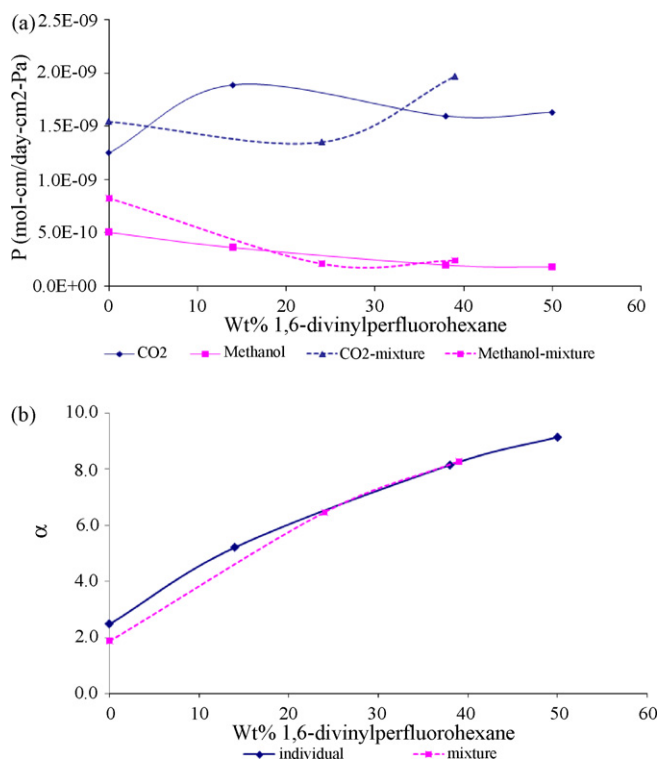


Fig. 8. (a) Permeability coefficient through PDMS and 1,6-divinylperfluorohexane composite. (b) Selectivity through PDMS and 1,6-divinylperfluorohexane.

Table 2  
Permeability coefficients (mol cm cm<sup>-2</sup> day<sup>-1</sup> Pa<sup>-1</sup>) and  $\alpha$  value of methanol and CO<sub>2</sub> through PDMS and PTMSP membranes

	PDMS		PTMSP	
	Individual setup	Binary setup	Individual setup	Binary setup
CO <sub>2</sub>	9.50E-10	1.60E-09	1.25E-09	1.70E-09
Methanol	4.80E-10	9.05E-10	5.10E-10	8.00E-10
$\alpha$	1.98	1.77	2.45	2.13



**Fig. 9.** (a) Permeability coefficient through PTMSP and 1,6-divinylperfluorohexane composite. (b) Magnitude of  $\alpha$  through PTMSP and 1,6-divinylperfluorohexane composite.

and b correspond to the results for CO<sub>2</sub> and methanol, and the dotted lines are for CO<sub>2</sub> and methanol mixtures. Fig. 8 shows that as the amount of 1,6-divinylperfluorohexane increases in the PDMS matrix, the permeability coefficient of CO<sub>2</sub> increases while that for methanol decreases, as shown by the solid lines. The permeability of CO<sub>2</sub> and methanol, when measured separately, through a membrane composed of 35 wt% of 1,6-divinylperfluorohexane in PDMS is  $P_{\text{CO}_2} = 1.8 \times 10^{-9} \text{ mol cm cm}^{-2} \text{ day}^{-1} \text{ Pa}^{-1}$  and  $P_{\text{MeOH}} = 5 \times 10^{-10} \text{ mol cm cm}^{-2} \text{ day}^{-1} \text{ Pa}^{-1}$ . This corresponds to a value of  $\alpha$  of 3.6, which is about twice that of the pure PDMS membrane. However, the permeability coefficient and  $\alpha$  trends when CO<sub>2</sub> and methanol were measured as mixtures did not comply with the independent measurement trend. It was observed that for CO<sub>2</sub> and methanol mixtures, the permeability coefficients of methanol increased at approximately the same rate as CO<sub>2</sub> for all compositions of PDMS and 1,6-divinylperfluorohexane. As a result, the values of  $\alpha$  for the polymer blend remained constant around 2.0.

Next, the performance of PTMSP and 1,6-divinylperfluorohexane blends as membrane candidates for CO<sub>2</sub> vent were studied. Permeation rates of methanol and CO<sub>2</sub> were obtained by themselves and in CO<sub>2</sub> and methanol mixtures. In these experiments, the PTMSP blends had an average thickness of 11  $\mu\text{m}$  and area of 2.85 cm<sup>2</sup>. In each case, the fluxes of CO<sub>2</sub> and methanol were measured and the permeability coefficients and  $\alpha$  values were calculated. Fig. 9a and b shows the permeability coefficients and  $\alpha$  of CO<sub>2</sub> and methanol through the polymer blend. The solid lines in these figures correspond to the results when the molecules were measured independently and the dotted lines correspond to the values obtained for mixtures of CO<sub>2</sub> and methanol. In both kinds of experiments, the permeability coefficient of CO<sub>2</sub> increased as the concentration of 1,6-divinylperfluorohexane in the polymer increased while the per-

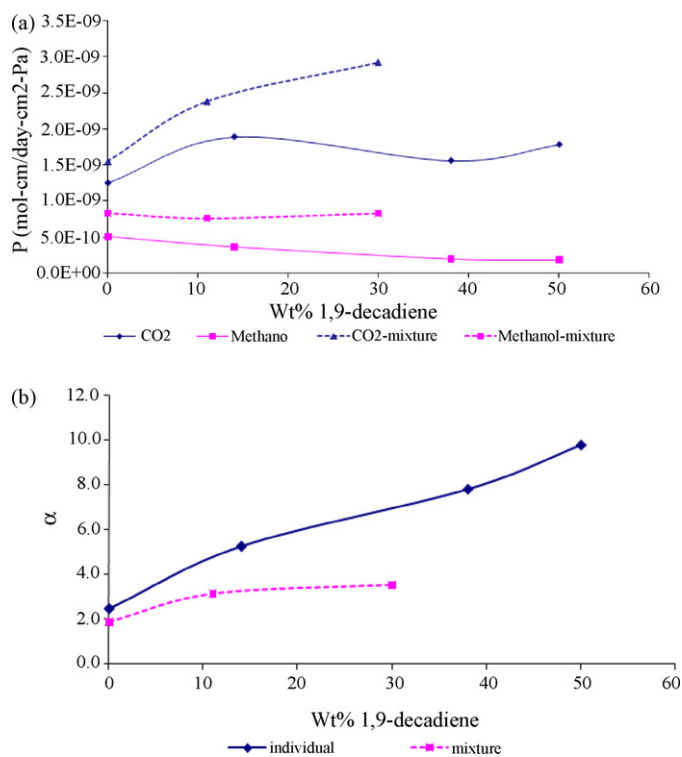


**Fig. 10.** (a) Permeability coefficient through PTMSP and 1,9-decadiene composite. (b) Magnitude of  $\alpha$  through PTMSP and 1,9-decadiene composite.

meability coefficient for methanol decreased. The permeability coefficient and  $\alpha$  trends when CO<sub>2</sub> and methanol were measured separately matched the values obtained for the mixtures. At 50 wt% of 1,6-divinylperfluorohexane in PTMSP, the CO<sub>2</sub> permeability coefficient was  $1.6 \times 10^{-9} \text{ mol cm cm}^{-2} \text{ day}^{-1} \text{ Pa}^{-1}$  and methanol was  $1.8 \times 10^{-10} \text{ mol cm cm}^{-2} \text{ day}^{-1} \text{ Pa}^{-1}$ . As a result,  $\alpha = 9.2$ , which was almost five times higher than the neat PTMSP membrane.

Since PTMSP blends showed higher permeability coefficients than PDMS and its mixtures, the addition of a second additive, 1,9-decadiene in PTMSP matrix was investigated. Like previous experiments, the rate of transport of methanol and CO<sub>2</sub> was measured by the independent and the binary system setups. In this case, membranes with average thickness of 120  $\mu\text{m}$  were cast and the flux of CO<sub>2</sub> and methanol were measured at STP across an area of 2.85 cm<sup>2</sup>. Fig. 10a and b shows both the permeability coefficients and  $\alpha$  for CO<sub>2</sub> and methanol as a function of 1,9-decadiene content in the PTMSP blend. The solid lines in Fig. 10 are for CO<sub>2</sub> and methanol measured separately and the dotted lines are for CO<sub>2</sub> and methanol in a mixture. The 1,9-decadiene/PTMSP membranes shows somewhat different permeabilities for the neat chemicals and their mixtures. For the separate permeability measurements of CO<sub>2</sub> and methanol, the permeability coefficient of carbon dioxide slightly increases with increasing 1,9-decadiene content while the permeability coefficient of methanol through the film appears to be significantly hindered. Thus,  $\alpha$  steadily increases with increased 1,9-decadiene in the polymer film. The largest  $\alpha$  obtained with this blend, 9.0, occurred with a 50:50 wt% mixture. However, the behavior observed for the vapor phase mixture of CO<sub>2</sub> and methanol was entirely different. In this case, the carbon dioxide permeation rate increased drastically with the addition of 1,9-decadiene and the methanol permeation rate was nearly unchanged. Therefore, the obtained  $\alpha$  was significantly reduced and the maximum value measured was 3.0 with 30 wt% 1,9-decadiene.

## 5. Discussion

The performance of PDMS and PTMSP polymer membranes as a selective CO<sub>2</sub> vent material has been demonstrated in this study. The permeability coefficients of CO<sub>2</sub> and methanol as pure species and as a non-ideal mixture through the polymer membranes were estimated. The results obtained from the permeability experiments of pristine PDMS and PTMSP membranes (Figs. 2, 3, 5 and 6) have been summarized in Table 2. It was observed that the overall permeability coefficient of CO<sub>2</sub> was higher than methanol for both the PDMS and the PTMSP membranes. The results shown in Table 2 shows that both membranes are hydrophobic in nature and allow the transport of CO<sub>2</sub> molecules with less hindrance than the polar, hydrophilic methanol molecules. It was also observed that the PTMSP membranes showed higher values for  $\alpha$  in comparison to the PDMS membranes.

The higher value of  $\alpha$  obtained for PTMSP membranes emphasizes the differences in the polymer structure of the PDMS and PTMSP membranes and their relative hydrophobicity. The higher permeability coefficients of CO<sub>2</sub> observed for the PTMSP membranes are because of the four methyl groups attached to each repeat unit in the PTMSP monomer in comparison to the two methyl groups in the PDMS monomer. As a result, hydrophilic methanol molecules experience added hindrance in their transport through the PTMSP membranes than through the PDMS membranes thereby generating higher values for  $\alpha$ .

The higher permeability coefficients obtained through PTMSP may also be due to its higher free volume. Unlike the PDMS matrix, PTMSP has alternating double bonds and a tertiary silicon moiety that causes unsymmetrical monomer packing in the matrix. Consequently, the PTMSP matrix has a lower polymer density (or high free volume density) than the PDMS matrix (0.75 g cm<sup>-3</sup> vs. 1.227 g cm<sup>-3</sup>). Another feature that distinguishes the permeation properties and void density of the PTMSP membranes from the PDMS membranes is its glassy nature. PTMSP is considered as a glassy polymer because of its high glass transition temperature (>200 °C). Conventionally, the highly rigid structure associated with glassy polymers should restrict the transport of permeates through it. However, unlike traditional glassy polymers, PTMSP exhibits extremely large gas permeabilities that are in some cases several orders of magnitude higher than otherwise expected. This behavior can be explained on the basis of the dual mode sorption theory [21]. According to this theory, glassy polymers consist of mixed matrix structure where “dense” regions of intertwined, tangled polymer chains exist with micro-voids scattered amongst them. Because of the low enthalpy of sorption associated with PTMSP and weak sorption properties, it is believed that the density of micro-voids in the PTMSP is very high [13]. Unlike rubbery polymers, where the transport mechanism of permeate is mostly a result of the diffusion and sorption, glassy polymers act as sieving media and allow for a size-selective transport mechanism. In this mechanism the transport of a species through the membrane is strongly influenced by the size of the penetrants and the number of micro-voids available in the transport pathway. Since the transport mechanism is a size-related fundamental property, it is evident that the PTMSP backbone with a continuum of micro-voids will show a higher permeability coefficient for CO<sub>2</sub> than the PDMS membrane while their hydrophobic end groups will ensure low permeability coefficients for methanol.

In the independent permeation experiments, Fig. 8a and b, the permeability coefficients of CO<sub>2</sub> increases while that of methanol decreases as a function of the 1,6-divinylperfluorohexane content in the PDMS membrane. This is likely due to the fact that the PDMS polymer blends are more hydrophobic than the pristine PDMS due to the addition of 1,6-divinylperfluorohexane. As a result, higher permeability coefficients of CO<sub>2</sub> and lower perme-

ability coefficients of methanol are expected. Previous studies by Sohn et al. have shown that in a polymer matrix with relatively high cross linking density, permeability is dictated by the diffusion of species thorough the polymer [22]. Because of the “mutually alike” nature of fluorinated PDMS matrix and CO<sub>2</sub>, its permeability coefficient increases. The polar methanol molecules (electron withdrawing/proton donating) have a tendency to form hydrogen bonds with their neighboring atoms. Thus, they aggregate together forming clusters of methanol. This observation has also been studied in the work done by Favre et al., who supported the cluster formation of methanol molecules and have suggested the non-random mixing between permeate-polymer or the degree of clustering depends on the solvent properties [21]. The authors have observed a high degree of clustering for methanol molecules, which explains their low diffusion coefficients and low solubility coefficients. Not only does the hydrophilic methanol suffer from the formation of large clusters, but it also suffers from a more tortuous path for transport through the hydrophobic fluorinated sites of the PDMS matrix. As a result, methanol molecules suffer from lower permeability coefficients through the fluorinated PDMS membranes.

However, unlike the individual permeability coefficients, the permeability coefficients of methanol and CO<sub>2</sub> in the binary experiments increased at the same rate, when both species were present in a mixture. The disparity observed in the trends of the methanol permeability coefficient between the individual and the binary system setups can be explained based on the interaction (attraction/repulsion) between the transporting moiety and the polymer matrix. It is likely that the swelling of the polymer membranes upon being exposed to methanol vapors provides an easier route for the transport of the bigger methanol clusters. In this case, one species with relatively similar properties as the polymer matrix could drag the other non-similar species with it, much like CO<sub>2</sub> dragging methanol clusters. Hence, a similar increase in the rates of mass transport for methanol and CO<sub>2</sub> were observed.

In the study of PTMSP blends with 1,6-divinylperfluorohexane, the permeability coefficients of CO<sub>2</sub> increased as a function of the additive content in the blend and that for methanol decreased, as shown in Fig. 9a and b. The trends of the permeability coefficients of the two species remained the same in both individual and the binary experiment setups, thereby emphasizing on the accuracy of the membrane vent performance under fuel cell conditions. Interestingly, while the difference in the permeability coefficients of CO<sub>2</sub> between pure PTMSP membrane and PTMSP with 40% 1,6-divinylperfluorohexane membrane is about 4%, the difference between the methanol permeability coefficients for the two membranes is 75%. Thus, the rise in  $\alpha$  that were observed in polymer blends of PTMSP with 1,6-divinylperfluorohexane are affected more by the greater decline in the permeability coefficient of methanol than by the permeability coefficient of CO<sub>2</sub>.

The lower permeability coefficient of methanol through all compositions of PTMSP and 1,6-divinylperfluorohexane is due to its polarity and the relatively larger size of methanol molecule clusters in comparison to CO<sub>2</sub>. The average void size in PTMSP matrix is 3.3 Å, as has been previously reported [13]. The average diameter of methanol molecule is 6.5 Å, which is more than two times the size of the void present in PTMSP. Moreover, as has been discussed before, methanol molecules tend to form large clusters due to the intra-molecular hydrogen bonding and as a result the relative size of the molecules becomes larger. Since it is known that the diffusion coefficient is proportional to the square of the difference in the penetrants size and the gap size of the pore, it is apparent that because of its larger size in comparison to the pore size of PTMSP, methanol molecules have lower transport through the matrix [13]. As a result, methanol molecules have lower permeability coefficients than CO<sub>2</sub>. Furthermore, upon addition of

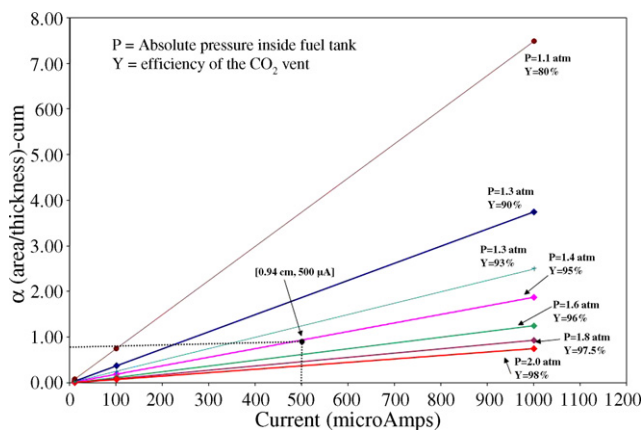


Fig. 11. Design specification of CO<sub>2</sub> vent and their efficiency ( $\gamma$ ).

1,6-divinylperfluorohexane, the pore size not only becomes smaller, but it also creates more hydrophobic sites due to the presence of a large number of fluorine atoms. Consequently, the methanol permeability coefficient declines continuously as the weight percent of the additive increases. Therefore, due to the high CO<sub>2</sub> permeability and the continuously decreasing methanol permeability, the values of  $\alpha$  is observed to increase with increasing amount of the additive in the polymer blend.

The similarity between the binary and the independent permeation experiments for PTMSP and 1,6-divinylperfluorohexane polymer blends was not observed in the PDMS and 1,6-divinylperfluorohexane blends. In the case of PTMSP and its composites, the transport mechanism was dictated predominantly by the free volume available in the matrix and the relative size of the permeating molecule. While in PDMS composite membranes, the methanol molecules could be more easily dragged through the matrix by CO<sub>2</sub> molecules. In the PTMSP composite membrane, the size of micro-voids restricts the rate at which methanol gets transported through. Thus, the permeability coefficients remain unaltered in the binary system and the trend in both cases is the same for the PTMSP blends.

The performance of the second additive, 1,9-decadiene, in PTMSP membranes is shown in Fig. 10a and b. It was observed that the permeability coefficient trends for the mixture of CO<sub>2</sub> and methanol were different than their individual permeability coefficients. It is observed that for the mixed systems, as the amount of additive in the matrix is increased, the permeability coefficients of methanol increased along with CO<sub>2</sub>. As a result the  $\alpha$  value is muted, much unlike the independent experiment setup. It is likely that due to the presence of longer chains of 1,9-decadiene, more flexibility was imparted to the PTMSP backbone. Therefore, the mechanism of methanol being dragged with CO<sub>2</sub> faced less hindrance, which reflected a more facile transport mechanism when both methanol and CO<sub>2</sub> were present together. As a result, the high values of  $\alpha$  that were observed in the independent setup is not replicated in the binary setup, and the blend cannot be considered as an optimum choice for CO<sub>2</sub> vent material.

In the above sections, the permeation behavior of CO<sub>2</sub> and methanol through different hydrophobic blends of PDMS and PTMSP membranes was studied. The best performing CO<sub>2</sub> vent was a polymer matrix with a 1:1 wt% of PTMSP and 1,6-divinylperfluorohexane with an  $\alpha$  value of 9.2. It was also observed that the performance of this membrane remained constant when both methanol and CO<sub>2</sub> were present as a non-ideal mixture which yielded the top performance under fuel cell operating conditions. Based on these values, a CO<sub>2</sub> vent for a passive, stand-alone DMFC was designed. The only parameter to be considered for the selec-

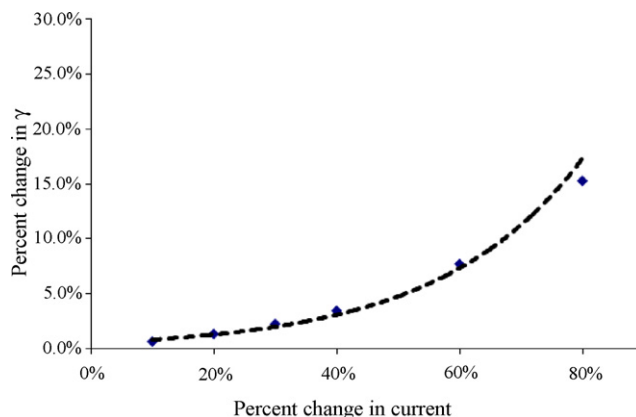


Fig. 12. Sensitivity of  $\gamma$  to changes in operating current.

tive CO<sub>2</sub> vent is its aspect ratio (area-to-thickness ratio). Thus, three independent variables: pressure, current, and membrane aspect ratio ( $\lambda$ ) fully define the fuel cell operating parameters and vent efficiency (fractional loss of methanol through the vent with respect to transport of all carbon dioxide and methanol through the vent).

At steady state, the rate of electrochemical oxidation of methanol is equal to the rate of CO<sub>2</sub> permeation through the film. Therefore, the membrane aspect ratio ( $\lambda$ ) is directly proportional to the operating current of a fuel cell and the rate of permeation of CO<sub>2</sub> through the membrane, as shown in the following equation:

$$\frac{i}{nF} = N_{\text{CO}_2} = P_{\text{CO}_2} p_{\text{CO}_2} \lambda \quad (12)$$

where  $p_{\text{CO}_2}$  is the absolute overpressure of CO<sub>2</sub> in the fuel container and  $\lambda$  is the aspect ratio of the film. Given that there are three variables in Eq. (12),  $i$ ,  $p_{\text{CO}_2}$  and  $\lambda$ , it is helpful to parametrically adjust one and plot the other two. Since the membrane efficiency is a function of selectivity, which is linearly related to the pressure, isobaric lines on an  $i$ - $\lambda$  curve would establish constant efficiency ( $\gamma$ ) trends. This relationship is shown in the following equation and plotted in Fig. 11.

$$\lambda = \left( \frac{1}{nFP_{\text{CO}_2} p_{\text{CO}_2}} \right) i \quad (13)$$

Fig. 11 shows the design conditions for a passive DMFC relating the operating current with CO<sub>2</sub> vent aspect ratio at a desired efficiency. This design specification plot was generated using the experimental results for 1:1 mixture of PTMSP and 1,6-divinylperfluorohexane where  $\alpha$  was equal to 9. Again, each solid line in Fig. 11 corresponds to the absolute pressure in the DMFC fuel tank. Using the line corresponding to a chosen pressure and a known value of the operating current, we can obtain the aspect ratio, selectivity and efficiency for the CO<sub>2</sub> vent. For example, if a direct methanol fuel cell operates at 500  $\mu\text{A}$  output current, and the allowed pressure inside the tank equals 1.4 atm (1400 kPa), the corresponding aspect ratio ( $\lambda$ ) for the vent design will be 0.94 cm. The fuel efficiency of the CO<sub>2</sub> vent or  $\gamma$  in this cell is 95%, meaning that only 5% of the consumed fuel is lost through the vent and a CO<sub>2</sub> selectivity of 19. Based on the value of  $\gamma$  of the vent, we can correctly size the fuel tank to provide for a specific mission life.

For this particular example, a fuel tank with 2 cm<sup>3</sup> of 12M methanol will allow the stand-alone DMFC to operate at 500  $\mu\text{A}$  for approximately a period of 1 year without refueling. Thus, the inclusion of a CO<sub>2</sub> vent in a stand-alone DMFC helps to size the fuel reservoir. The effect of changes in operating current ( $i$ ) on  $\gamma$ , keeping a constant aspect ratio ( $\lambda$ ) is shown in Fig. 12. The curve shown in Fig. 12 shows that even if the operating current

of a passive DMFC decreased by 20%, the efficiency of the vent would exhibit a 1.4% decline. This implies that if a passive DMFC designed to operate at 500  $\mu$ A experiences an abrupt change in current (e.g. 20% decline), the vent will release CO<sub>2</sub> with 93.6% efficiency and maintain the pressure inside the fuel tank at 1.32 atm. As such, the passive DMFC will not experience a burst in pressure that would have otherwise resulted in significant damages to the DMFC through increased methanol crossover, sealant ruptures and decreased its performance and lifetime.

## 6. Conclusions

The permeation behavior of CO<sub>2</sub> and methanol through various compositions of PDMS and PTMSP membranes with 1,6-divinylperfluorohexane and 1,9-decadiene additives were studied. The results presented in this study indicate that both PDMS and PTMSP membranes were more selective towards CO<sub>2</sub> permeation than methanol. It was also observed that under the same experimental conditions, PTMSP membranes showed higher intrinsic selectivity ( $\alpha$ ) than the PDMS membranes. The better performance of the PTMSP membranes was mostly due to the presence of four hydrophobic methyl groups in each repeat unit that hindered the transport of hydrophilic methanol clusters. Furthermore, upon the addition of 1,6-divinylperfluorohexane, both PDMS and PTMSP membranes exhibited higher selectivity towards the transport of CO<sub>2</sub> than methanol. The permeation trends of CO<sub>2</sub> and methanol through all compositions of PTMSP and 1,6-divinylperfluorohexane remained unchanged when both moieties were present as mixture, much like a fuel cell operating condition. The best performance was obtained with 50 wt% of 1,6-divinylperfluorohexane in PTMSP membrane, such that the permeability coefficient of CO<sub>2</sub> was  $1.6 \times 10^{-9}$  mol cm cm<sup>-2</sup> day<sup>-1</sup> Pa<sup>-1</sup> and methanol was  $1.8 \times 10^{-10}$  mol cm cm<sup>-2</sup> day<sup>-1</sup> Pa<sup>-1</sup>. The corresponding  $\alpha$  was 9.2, which is approximately 5 times higher than pure PTMSP and 10 times higher than pure PDMS membranes. Based on these results a stand-alone DMFC with CO<sub>2</sub> vent was designed. The dependence of the membrane aspect ratio ( $\lambda$ ) on the fuel cell operating current has been demonstrated. It was observed that at a given aspect ratio, the efficiency of a CO<sub>2</sub> vent ( $\gamma$ ) had limited sensitivity towards abrupt changes in current. As a result, the novel CO<sub>2</sub> vent can tolerate unforeseen bursts in pressure due to changes in current without having a drastic impact on the fuel cell design and performance.

## Acknowledgements

The authors would like to thank the Test Resource Management Center (TRMC) Test and Evaluation/Science and Technology (T&E/S&T) Program for their support. This work is funded by the T&E/S&T Program through the Naval Undersea Warfare Center, Newport, RI, contract number N66604-06-C-2330. The authors would also like to acknowledge the financial contributions of WiSPI.net and the Georgia Research Alliance.

## References

- [1] X. Li, Principles of Fuel Cells, Taylor & Francis group, New York, 2006.
- [2] P. Agnolucci, International Journal of Hydrogen Energy 32 (2007) 4319–4328.
- [3] S. Motokawa, M. Mohamedi, T. Momma, S. Shoji, T. Osaka, Electrochemistry Communications 6 (2004) 562–565.
- [4] G.Q. Lu, C.Y. Wang, T.J. Yen, X. Zhang, Electrochimica Acta 49 (2004) 821–828.
- [5] J. Li, C. Moore, P.A. Kohl, Journal of Power Sources 138 (2004) 211–215.
- [6] J. Li, C.W. Moore, D. Bhusari, S. Prakash, P.A. Kohl, Journal of the Electrochemical Society 153 (2006) A343–A347.
- [7] C.W. Moore, Microfabricated Fuel Cells to Power Integrated Circuits, PhD dissertation, Georgia Institute of Technology, Atlanta, 2005, p. 210.
- [8] C.W. Moore, J. Li, P.A. Kohl, Journal of the Electrochemical Society 152 (2005) A1606–A1612.
- [9] K. Wozniak, D. Johansson, M. Bring, A. Sanz-Velasco, P. Enoksson, Journal of Micromechanics and Microengineering 14 (2004) S59–S63.
- [10] H. Yang, T.S. Zhao, Q. Ye, Journal of Power Sources 139 (2005) 79–90.
- [11] S.C. Kelley, G.A. Deluga, W.H. Smyrl, AiCHE Journal 48 (2002) 1071–1082.
- [12] A. Blum, T. Duvdevani, M. Philosoph, N. Rudoy, E. Peled, Journal of Power Sources 117 (2003) 22–25.
- [13] W.J. Koros, G.K. Fleming, Journal of Membrane Science 83 (1993) 1–80.
- [14] S.M. Jordan, W.J. Koros, Journal of Polymer Science Part B–Polymer Physics 28 (1990) 795–809.
- [15] C.M. Zimmerman, A. Singh, W.J. Koros, Abstracts of Papers of the American Chemical Society 215 (1998) U326–U1326.
- [16] M.V. Chandak, Y.S. Lin, W. Ji, R.J. Higgins, Journal of Applied Polymer Science 67 (1998) 165–175.
- [17] K. Efimenko, J.A. Crowe, E. Manias, D.W. Schwark, D.A. Fischer, J. Genzer, Polymer 46 (2005) 9329–9341.
- [18] A.L. Hines, R.N. Maddox, Mass Transfer: Fundamentals and Applications (1985).
- [19] J. Comyn (Ed.), Polymer Permeability, Elsevier, London & New York, 1985.
- [20] J. Crank, The Mathematics of Diffusion, 2nd ed., Oxford University Press, USA, 1975.
- [21] E. Favre, P. Schaetzel, Q.T. Nguyen, R. Clement, J. Neel, Journal of Membrane Science 92 (1994) 169–184.
- [22] W.I. Sohn, D.H. Ryu, S.J. Oh, J.K. Koo, Journal of Membrane Science 175 (2000) 163–170.